Efficient and Fast Active Equalization Method for Retired Battery Pack Using Wide Voltage Range Bidirectional Converter and DBSCAN Clustering Algorithm

Wang Lujun, Ke Jinyang, Zhan Min, Tian Aina, Wu Tiezhou, Zhang Xiaoxing, and Jiang Jiuchun, *Senior Member, IEEE*

***Abstract*—This article presents an efficient and fast echelon battery equalization method based on wide voltage range bidirectional converter combined with *DBSCAN (density-based spatial clustering of applications with noise)* clustering control strategy. Thanks to the wide voltage range and bidirectional buck-boost characteristics of the four-switch bidirectional converter, the battery energy can be reasonably redistributed between the battery and the super capacitor. The converter operating in synchronous rectification mode can not only achieve bidirectional energy flow in a wide voltage range, but also has a high energy conversion efficiency. The *DBSCAN* clustering algorithm is used to divide all battery cells into groups, and each group may contain one or more adjacent and nonadjacent battery cells. First, the nonadjacent single cells are balanced and integrated into adjacent group with the closest voltage. Then, the groups with different voltages are balanced by group-to-group, thereby realizing rapid balance of the entire battery pack. In order to verify the effectiveness of the proposed method, simulations and experimental verification were carried out. The experimental results show that, comparing with traditional battery balancing methods, the proposed method achieves shorter balancing time and higher balancing efficiency.**

***Index Terms*—Active equalization circuit, battery pack, *DBSCAN* clustering algorithm, four-switch bidirectional converter, super capacitor.**

I. Introduction

FACING the dual pressure of energy and environment, new energy vehicles represented by electric vehicles are developing rapidly [1]–[3]. Lithium batteries have become the main energy source for electric vehicles thanks to their low self-discharge rate, high energy density, and long cycle life [4], [5]. After a few years use of electric vehicles, a large number of lithium batteries will be retired, therefore government and battery manufacturers are facing tremendous pressure on battery recycling and disposal [6]. Generally speaking, the capacity of retired lithium-ion power batteries still has 70% to 80% of its initial capacity. After retesting and classification, some retired batteries can still be used for energy storage in the power grid [7], [8].

As the retired battery has been used for a long time, the inconsistency among each individual retired battery pack is more obvious than that of the battery pack in service. Larger inconsistencies will reduce the available capacity of the battery pack, shortening the cycle life, and may cause safety problems due to overcharging and over-discharging [9], [10]. Therefore, it is very critical to balance the battery pack when reusing retired battery.

Battery equalization technology is usually divided into passive equalization and active equalization. Among them, passive equalization technology is an energy-consumption type equalization technology, which consumes excessive battery energy by adding energy-consuming components to achieve battery balancing. Passive equalization technology has the advantages of simple method and low cost, but it has shortcomings such as large loss, low energy utilization, and slow equalization speed. In addition, the temperature rise of the battery pack caused by energy consumption during the equalization process may cause a thermal runaway of the battery pack [11]. Therefore, passive equalization is not suitable for the balancing of decommissioned batteries. Active equalization, as a nonenergy-consuming equalization, can transfer the excess energy of the battery to the battery with lower energy in the battery pack through the equalization element, thereby achieving the balance of the entire battery pack [12]. Compared with passive equalization, active equalization has the advantages of higher energy utilization, smaller battery pack temperature rise, and faster equalization speed [13]. Therefore, active balancing technology has become the first choice for balancing retired batteries.

According to the type of energy storage elements in the balancing process, active equalization methods can be divided

Manuscript received 17 November 2021; revised 24 January 2022 and 27 April 2022; accepted 9 June 2022. Date of publication 22 June 2022; date of current version 26 July 2022. This work was supported by the National Natural Science Foundation of China under Grant 51607060. Recommended for publication by Associate Editor D. Vinnikov. *(Corresponding author: Jiang Jiuchun.)*

The authors are with the Department of Hubei Key Laboratory for High-efficiency Utilization of Solar Energy and Operation Control of Energy Storage System, Hubei University of Technology, Wuhan 430068, China (e-mail: wanglujun@zju.edu.cn; 101900167@hbut.edu.cn; 102010285@hbut.edu.cn; ainatian@hbut.edu.cn; wtz315@163.com; zhangxx@hbut.edu.cn; jcjiang@bjtu.edu.cn).

Color versions of one or more figures in this article are available at https://doi.org/10.1109/TPEL.2022.3185242.

Digital Object Identifier 10.1109/TPEL.2022.3185242

into subcategories of circuit topologies based on capacitances [14]–[16], inductances [17]–[19], transformers [20]–[22], and dc–dc converters [23], [24]. The balancing method based on capacitance mainly uses the voltage difference between each single cell and the principle that the voltage at both ends of the capacitor cannot change abruptly to realize the battery energy handling. Shang *et al.* [14] propose a switched capacitor equalizer using capacitors as the energy carriers in the equalization process, the energy in each cell can be flexibly carried between cells to achieve the balance of the battery pack. However, the smaller equalization current results in a slower balancing speed. In contrast to capacitance-based equalization methods, inductance-based balancing method uses inductors as energy storage elements, and battery energy is transferred in the form of current. Phung *et al.* [17] propose an inductor-based equalizer to solve the imbalance problem between cells. This equalization method uses inductors as energy carriers to achieve energy transfer between cells, and the equalization speed is faster. However, the balance efficiency is low and the presence of a large number of inductors is not conducive to safe and stable operation of the circuit. The transformer-based balancing method uses the multiwinding transformer as the main body of the equalizer, and each battery is connected to a winding of the transformer. Li *et al.* [20] propose a modular equalizer using a multiwinding transformer. The multiwinding transformer is used as the main body of the equalizer, and the overall balance of the battery pack is finally achieved through the energy transfer between the single cell and the battery pack. This method can quickly achieve the balance between each single cell, but each cell needs to be connected to a transformer winding, which makes the equalizer more expensive when the number of cells increase. The balancing method based on dc–dc converters is an equalization method that uses dc–dc converter as the main body of the equalizer. Kim *et al.* [13] propose a modularized equalizer based on the two-stage dc–dc converter. The energy of the battery pack is transferred to the battery with lower energy through the two-stage dc–dc converter, and finally the energy of each cell in the pack tends to be balanced. However, the structure of this method is complex and it is difficult to control. In addition, the voltage ripple and current ripple caused by the converter will also affect the battery energy transfer [25]. Therefore, the use of a reliable and efficient converter as the equalization body is fundamentally important for improving the equalization efficiency, equalization time, and equalization safety of the decommissioned battery pack.

In order to solve the above-mentioned problems of the traditional balancing method, and reduce the inconsistency of the battery during the energy storage process of the retired battery, this article proposes an efficient and fast active equalization circuit using wide voltage range bidirectional converter and *DBSCAN (density-based spatial clustering of applications with noise)* clustering algorithm. The equalization circuit is composed of four-switch bidirectional converter, super capacitor, and switch matrix. Among them, the four-switch bidirectional converter can realize high flexibility and conversion efficiency. Cooperating with the compound balancing strategy of single to single and group to groups, the equalizer can reduce the energy loss during the equalization process and realize the efficient and fast equalization of the decommissioned battery pack.

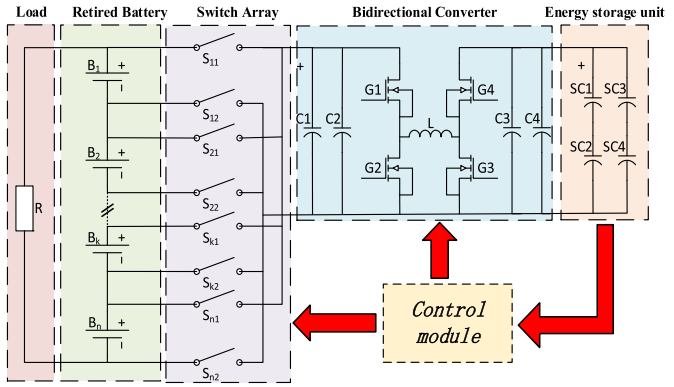

Fig. 1. Circuit topology of the proposed method.

The rest of this article is organized as follows. Section II introduces the equilibrium topology and circuit working principle. The equalization strategy and equalization algorithm corresponding to the equalization circuit is proposed in Section III. In Section IV, a simulation model of the equalization circuit was built on the MATLAB/Simulink platform, and the feasibility of the equalization method was verified through simulation. In Section V, a small equalization experiment platform has been created to carry out the converter efficiency test and the equalization effect test of the decommissioned battery pack, respectively, and the effectiveness of the equalization method is verified through the balancing experiment. Finally, Section VI concludes this article.

II. Topological Structure and Working Principle

A. Balancing Topology

In order to effectively realize the balancing of retired batteries, the balancing circuit shown in Fig. 1 is proposed. The circuit is composed of a lithium battery pack, a switch array, a four-switch synchronous bidirectional converter, and an energy transfer unit composed of super capacitor. The main functions of each part are described in detail as follows.

The positive pole of the single-cell battery inside the battery pack is connected to S_{n1}, and the negative pole is connected to S_{n2} (where n represents the serial number of corresponding battery). As shown in (1) and (2), the positive switch is connected to form a positive bus, and the negative switch is connected to form a negative bus.

$$Bus_{+} = \{S_{11}, S_{21}, \ldots, S_{n1}\} \tag{1}$$

$$Bus_{-} = \{S_{12}, S_{22}, \ldots, S_{n2}\}. \tag{2}$$

In (1) and (2), Bus_{+} represents the positive pole of the bus bar; Bus_{-} represents the negative pole of the bus bar. As shown in Fig. 1, the positive bus is connected to the positive pole of the four-switch bidirectional converter, and the negative bus is connected to the negative pole of the converter. This circuit structure can flexibly select any single battery cell of the battery pack or any battery pack cell connected in series with adjacent battery

cells to connect to the four-switch synchronous bidirectional converter.

The four-switch bidirectional converter works in the synchronous rectification mode, which ensures the higher conversion efficiency of the converter while realizing the bidirectional buck-boost, so as to realize the energy exchange between the battery pack and the energy storage unit. Since the four-switch synchronous bidirectional converter is a single-inductor structure, the design of the inductor needs to consider both boost and buck modes. For the Buck converter, when the converter output is fully loaded and the input voltage is the maximum, the inductor ripple is the largest, which should satisfy (3). For the Boost converter, when the input voltage is the smallest, the ripple of the inductor is the largest, which should satisfy (4).

$$\Delta I_L = \frac{V_{out}}{f_s \cdot L} \cdot \left(1 - \frac{V_{out}}{V_{in(\max)}}\right) \tag{3}$$

$$\Delta I_L = \frac{V_{in(\min)}}{f_s \cdot L} \cdot \left(\frac{V_{out} - V_{in(\min)}}{V_{out}}\right). \tag{4}$$

In (3) and (4), ΔI_L represents the inductor current ripple; f_s represents the frequency of the main switch; V_{out} represents the output voltage; L represents the value of inductance; $U_{in(max)}$ represents the maximum input voltage value; $U_{in(min)}$ represents the minimum input voltage.

It can be seen that the maximum inductor ripple is determined by the maximum input voltage and the minimum input voltage at the same time, so the inductor ripple coefficient should be selected as a compromise. In the boost mode, when the input voltage is the smallest, the maximum inductor current ripple coefficient is 0.2-0.3. In the step-down mode, when the input voltage is the maximum, the maximum inductor current ripple factor is 1-1.5. The inductor current ripple coefficient satisfies the following equation:

$$K_{ripple} = \frac{I_{Peak-Peak}}{I_{L(av)}}. \tag{5}$$

In (5), $I_{Peak\text{-}Peak}$ represents the peak-to-peak value of the inductor current; and $I_{L(av)}$ represents the average value of the inductor current. Combining (3)–(5) can calculate the converter inductance L.

In addition, the super capacitor *SC* is used as an energy storage unit in the equalization process of the decommissioned battery pack. Due to the advantages of high energy density, fast charging speed, long service life, and high charging and discharging efficiency of super capacitors, it can store and release the energy well during the balancing process, which is beneficial to improve the balancing efficiency.

B. Working Principal Analysis

The equalization variable is generally the battery voltage or the battery *SOC* value. The *SOC* value of the battery is used as an equilibrium variable, such as ampere-hour integration method, Kalman filtering, neural network, and other methods. Among them, the ampere-hour integration method cannot guarantee the accuracy of the estimation of the *SOC* value of the battery due to the inaccuracy of the branch current measurement. Methods such as Kalman filtering and neural network have high estimation accuracy, but the amount of calculation is large and not easy to implement. In contrast, the voltage is easy to measure and implement. Therefore, the battery voltage as an equalization variable is a more practical solution in the battery equalization control. This article chooses voltage as the equilibrium variable.

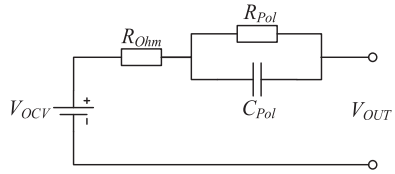

Fig. 2. Battery first-order RC model.

1) OCV Estimation of Retired Batteries: The parameters of the retired batteries are obtained through hybrid pulse power characteristic test, including internal resistance, polarization internal resistance, and polarization internal capacitance. According to the obtained parameters, the first-order RC model of the lithium battery is established as shown in Fig. 2.

In Fig. 2, V_{OCV} represents the open circuit voltage of the retired battery; R_{Ohm} represents the internal resistance of the battery; R_{Pol} represents the polarization internal resistance of the battery; C_{Pol} represents the polarization capacitance of the battery; and V_{OUT} represents the battery output voltage.

According to Kirchhoff's voltage law and Kirchhoff's current law, (6) and(7) can be obtained.

$$\mathrm{C}_{Pol}\frac{dV_{pol}}{dt} + \frac{V_{pol}}{R_{pol}} = I \tag{6}$$

$$V_{OUT} = V_{OCV} - IR - V_{pol}. \tag{7}$$

In (6) and (7), V_{Pol} is the polarization voltage of the battery (The voltage across R_{Pol} and C_{Pol}); and I is output current of the battery. Combining (6) and (7) to obtain the polarization voltage V_{Pol}, as shown in (8), where t_0 represents the initial time of battery charging and discharging.

$$V_{Pol}(t) = V_{pol}(t_0)e^{-\frac{t}{R_{pol}C_{pol}}} + IR_{pol}(1 - e^{-\frac{t}{R_{pol}C_{pol}}}) \tag{8}$$

$$V_{OCV} = V_{OUT} + IR + V_{pol}. \tag{9}$$

Combining (8) and (9), V_{OCV} of the decommissioned battery pack can be estimated.

2) Balancing Between Single Cells: The single cell equalization is performed on the retired battery pack when the voltage of the retired batteries satisfies the following equations:

$$V_{av} = \frac{V_1 + V_2 + \ldots + V_n}{n} \tag{10}$$

$$|V_n - V_{av}| \geq V_M. \tag{11}$$

In (10) and (11), V_{av} represents the average voltage of the battery pack; V_n represents the voltage of any single cell in the battery pack; and V_M represents the equilibrium threshold. The balancing is turned ON when the difference between V_n and V_{av} is greater than the balancing threshold V_M.

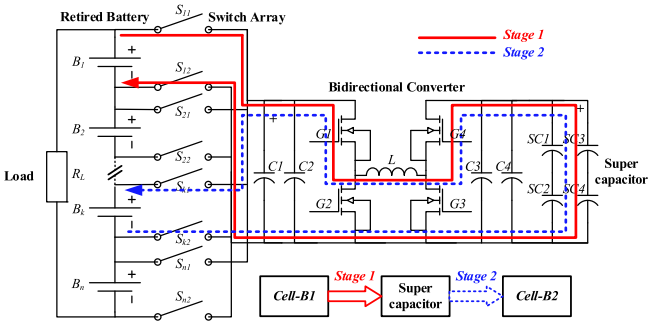

Fig. 3. Diagram of single battery balance.

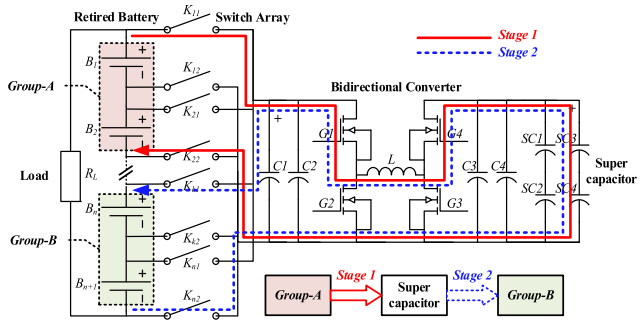

Fig. 4. Diagram of battery pack balance.

As shown in Fig. 3, the voltage of battery B_1 is higher, and the voltage of battery B_2 is lower. The excess energy of B_1 is transferred to battery B_2. The balancing process is carried out in the following two stages.

Stage 1: turn-OFF switches S_{11} and S_{12} to select the corresponding equalization path. Because the voltage of the single battery is lower than the set value of the super capacitor voltage, the four-switch bidirectional converter works in the synchronous boost state. The working condition of the converter is: switch *G1* is normally open, switch *G2* is normally closed, the main switch *G3* is controlled to work, and switch *G4* is controlled for synchronous rectification. The specific working conditions satisfy the following equation:

$$\frac{V_{SC}}{V_{BAT}} = \frac{1}{1-D}. \tag{12}$$

In (12), V_{SC} represents the voltage setting value of the super capacitor; V_{BAT} represents the voltage of a single battery; and D represents the duty cycle of the main switch. When the converter starts to work, energy flows from the battery B_1 and flows into the super capacitor for storage through the boost effect of the converter. When the voltage of the super capacitor reaches the voltage setting value, the equalizer ends the equalization stage 1.

Stage 2: turn-OFF switches S_{K1} and S_{K2} to select the equalization channel. Since the voltage of the super capacitor is greater than the voltage of the single battery B_2, the four-switch bidirectional converter works in a synchronous step-down mode. Switch *G4* is kept normally open, switch *G3* is kept normally closed, the main switch *G1* is controlled to work, and switch *G2* is controlled for synchronous rectification at the same time. The switch working conditions satisfy the following equation:

$$D = \frac{V_{SC}}{V_{Bat}}. \tag{13}$$

The bidirectional converter controls the flow of energy from the super capacitor SC into the battery B_1. When the capacitor voltage drops slowly to the minimum value, the equalization stage 2 ends.

Repeating the operations of stages 1 and 2 until the voltages of batteries B_1 and B_2 reach equilibrium.

3) Balancing Between Internal Groups: Considering the actual unbalanced condition in balancing process is more complicated, and the single processing of the battery is relatively cumbersome and low in efficiency. In this article, the batteries are internally grouped, and then the excess energy of the internal groups with higher energy is secondarily distributed to the internal battery pack with lower energy to improve the equalization speed of the entire battery pack.

As shown in Fig. 4, batteries B_1 and B_2 constitute *Group-A*, and batteries B_n and B_{n+1} constitute *Group-B*. Assuming that the energy of *Group-A* is higher than the energy of *Group-B*, the excess energy of *Group-A* will be transferred to *Group-B*. Similar to the balance between single cells, the internal group balance is divided into the following two stages.

Stage 1: selecting the equalization channel corresponding to *Group-A* through the switch matrix, and start the four-switch bidirectional converter. Since the voltage of *Group-A* is greater than the set value of the super capacitor voltage, the four-switch bidirectional converter works in a synchronous step-down mode, and the energy in *Group-A* is transferred to the super capacitor for storage through the converter. When the super capacitor voltage reaches the preset voltage value, stage 1 ends.

Stage 2: selecting the equalization channel corresponding to *Group-B* through the switch matrix, and start the four-switch bidirectional converter. Since the voltage on the super capacitor is lower than the voltage of *Group-B*, the converter works in a synchronous boost mode, and the energy in the super capacitor is reversely charged into *Group-B* through the converter. When the voltage of the super capacitor drops to the minimum value, stage 2 ends.

Repeating stages 1 and 2 until the energy of *Group-A* and *Group-B* reach equilibrium.

III. DBSCAN Equilibrium Control Strategy

A. Equilibrium Strategy

In order to simplify the complex balancing conditions in the actual balancing process of the decommissioned battery pack, and improve the overall balancing speed of the batteries, the *DBSCAN* cluster balancing control strategy is adopted to balance the decommissioned battery pack.

The *DBSCAN* cluster balance control strategy is to use the *DBSCAN* algorithm to perform a cluster search on the target unit, and use the cell voltage of the decommissioned battery pack as the clustering basis to perform cluster analysis on the battery cells of the battery pack. After the battery pack is classified, it is divided into two parts: adjacent series-connected internal

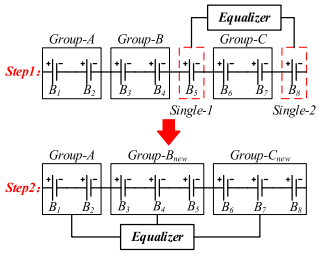

Fig. 5. Diagram of equalization algorithm.

battery pack units of the same voltage category and nonadjacent internal single battery units, as shown in Fig. 5.

B. Equilibrium Algorithm

Take the balance of n cell series retired lithium batteries as an example. The n batteries are marked as $[B_1,B_2,\ldots,B_n]$, the battery voltages are, respectively, marked as $[V_1,V_2,\ldots,V_n]$, and the average voltage V_{av} is shown in the following equation:

$$V_{av} = \frac{V_1 + V_2 + , \ldots , + V_n}{n}. \tag{14}$$

The difference between the single battery and the average voltage is e_i, calculated as shown in the following equation:

$$e_i = V_i - V_{av}. \tag{15}$$

The n-dimensional error vector $E[e_1,e_2,\ldots,e_n]$ can be obtained from (11). According to the error vector, the set G can be obtained as shown in the following equation:

$$G = \{(n_1, e_1), (n_2, e_2), \ldots , (n_x, e_x)\}. \tag{16}$$

In (16), e_x represents the error e between the battery voltage and the average voltage, and n_x represents the corresponding battery label.

Set the neighborhood parameters of the *DBSCAN* algorithm to (*eps*, *min_samples*), take the error value e_1 of the battery B_1 as the center of the circle, and use the given parameter eps as the radius to determine the containment area of the error value e_1. By judging whether the error value e_x of other batteries is within the inclusion area of e_1, the density value ρ_1 of battery B_1 can be determined. Compare the density value ρ_1 of battery B_1 with the neighborhood parameter *min_samples*. If $\rho_1 >$ *min_samples*, the error value e_1 of battery B_1 is defined as the core point. If $1 < \rho_1 <$ *min_samples*, the error value e_1 of battery B_1 is defined as the boundary point. If $\rho_1 = 1$, the error value e_1 of battery B_1 is defined as noise point.

The core points and boundary points are, respectively, subjected to the above-mentioned search process, until no new core points appear in the core point set, and then jump out to search for the next voltage category. The search steps are the same as the above-mentioned process.

After *DBSCAN* clustering of the entire battery pack, d number of clusters can be obtained $\{S_1,S_2,\ldots,S_d\}$, separate the nonadjacent battery cells in this cluster to form a new cluster, as shown in the following equation:

$$\{S_1, S_2, \ldots , S_d\} = \{N_1, N_2, \ldots , N_a\} + \{D_1, D_2, \ldots , D_b\}. \tag{17}$$

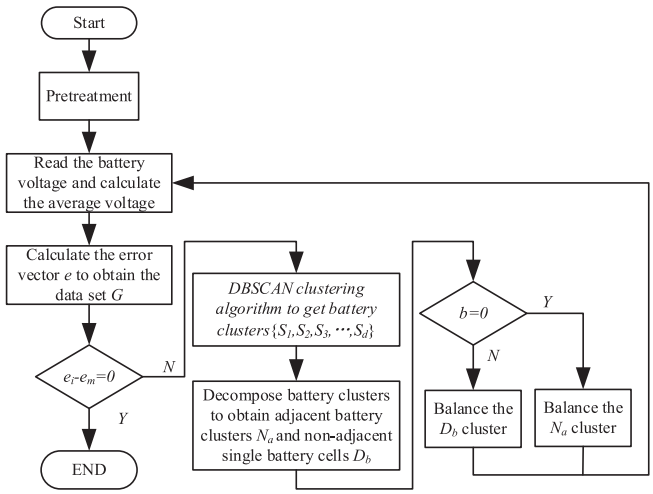

Fig. 6. Flowchart of the proposed cell balancing algorithm.

In (17), N_a represents a new cluster that excludes nonadjacent battery cells; D_b represents the nonadjacent battery cells; a represents the number of adjacent battery cells; b represents the number of nonadjacent battery cells.

Prioritize the equalization of nonadjacent battery cells, until the nonadjacent battery cells no longer appear in the clustering result, start the balancing between the clusters of the battery clusters, and finally achieve the balance of the battery packs. Fig. 6 is the flowchart of the algorithm.

The balance of nonadjacent single cells is mainly divided into the following two cases.

a) The voltage of nonadjacent single cell is greater than the average voltage of the nearest battery group. At this time, the single cell transmits energy to the cell or group with the lowest voltage, so that the single cell "integrates" into the division of the adjacent internal battery groups, and then starts the balancing of internal groups.

b) The voltage of nonadjacent single cell is less than the average voltage of the nearest battery group. At this time, the cell or group with the highest voltage transmits energy to the nonadjacent single cell until the single cell "integrate" into the division of the adjacent internal battery group, and then starts the balancing of internal groups.

IV. Simulation Results

A simulation model is constructed on the MATLAB/Simulink platform, as shown in Fig. 7. The simulation parameters are set as follows: the MOSFET switching frequency is 600 kHz, the converter inductance is 3.3 μH, the value of the super capacitor is 10 F/5.4 V, lithium battery nominal voltage is 3.7 V, battery internal resistance is 8 mΩ, battery rated capacity is 5.4 AH, the on-state resistance of MOSFET is 0.1 Ω, and the body diode conduction voltage drop is 0.8 V.

The battery pack are, respectively, subjected to equilibrium simulation in the resting state, charging state, and discharging state. The initial value of the battery is: $V_{b1} = 3.31$ V, $V_{b2} = 3.83$ V, $V_{b3} = 3.53$ V, $V_{b4} = 3.62$ V, $V_{b5} = 3.75$ V, and $V_{b6} = 3.36$ V.

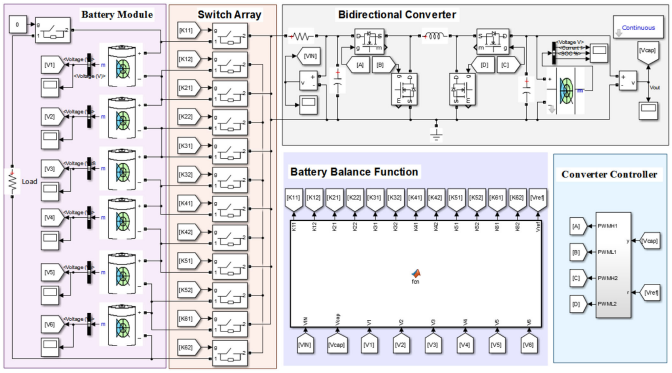

Fig. 7. Equilibrium simulation model.

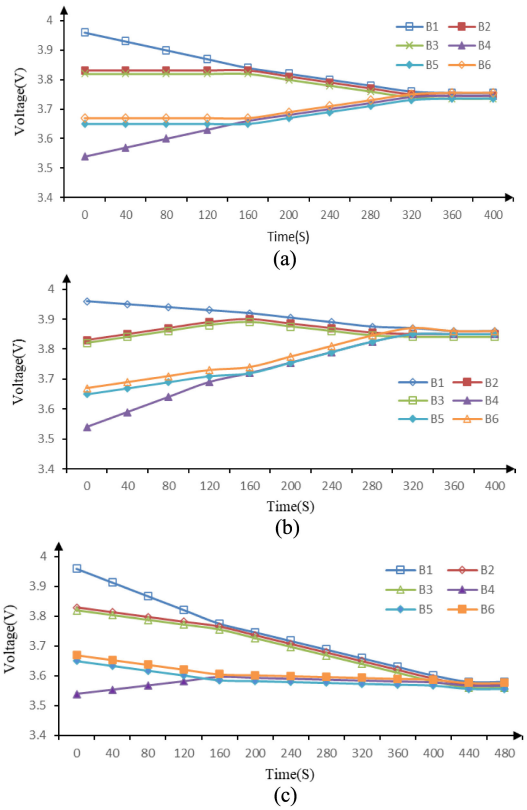

Fig. 8. Battery status under different equilibrium conditions. (a) Battery status under static equilibrium. (b) Battery status under charge equilibrium. (c) Battery status under discharge equilibrium.

Fig. 8(a) shows the equalization process of the battery pack in a static state. The figure shows that the battery pack has two internal sub-battery packs around 160 s, and basically reaches equilibrium around 320 s. Fig. 8(b) shows the voltage change of each battery in the battery pack in the charging state. As can be seen in the figure, in the charging state, the battery pack is basically balanced after 280 s. Fig. 8(c) shows the voltage change of each battery when the battery pack is balanced in the discharged state. As can be seen in the figure, the battery pack reaches an overall equilibrium state around 440 s.

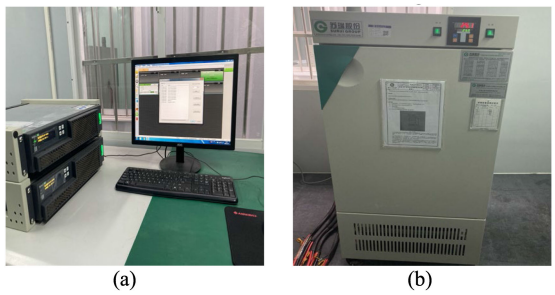

Fig. 9. Battery test equipment. (a) Battery tester. (b) Thermostat.

TABLE I
BATTERY REMAINING CAPACITY

Label	B1	B2	B3	B4	B5	B6
Capacity(mAh)	1870	1826	1860	1789	1756	1804

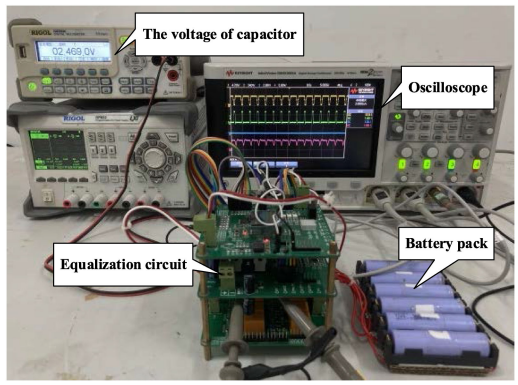

Fig. 10. Equilibrium experiment platform.

V. EXPERIMENTAL RESULTS

Before the start of the experiment, the remaining capacity of the battery will be tested by the battery tester. A thermostat is used to control the ambient temperature, and the temperature is set to 25 °C. The instrument is shown in Fig. 9.

The battery in the experiment has a nominal voltage of 4.2 V, a nominal capacity of 2200 mAh, and a battery model of 18650. The remaining capacity of each battery is shown in Table I.

It can be seen from Table I that the remaining capacity of the battery used for experiment is about 80% of the original nominal capacity.

To demonstrate the validity of the balancing system, a small balance prototype circuit was tested, as shown in Fig. 10. The prototype circuit consists of four parts: a series battery pack unit composed of used lithium-ion battery, a switch array unit, the main body of the equalizer composed of four-switch bidirectional converter and super capacitors, and a main control circuit with STC8 as the core.

The main control chip STC8 only contains 812-bit ADC interfaces, two of which are used for working current at both ends of the converter, and the remaining 6 ADC sampling ports are used for battery voltage sampling. Therefore, the series battery pack unit consists of 6 used 18650 batteries. In addition, the

TABLE II
PARAMETERS OF CIRCUIT

Components	Type	Parameter
Converter chip	SC8802QDER/QFN-32	
Main inductance	SMMS1040-3R3M	3.3 uH
Frequency		600 kHz
Diode	SS56/SMA	5A/60 V
MOSFET	NCE40H12/TO220	120 A/40 V/130 W
Super capacitor	HP-2R7-J106UY	10 F/2.7 V*4

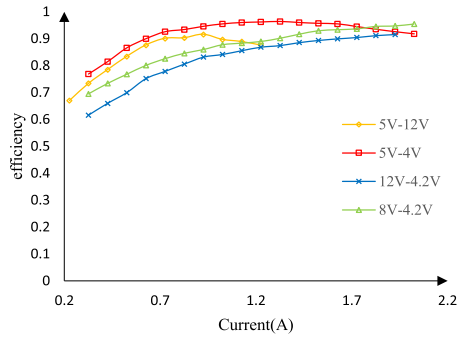

Fig. 11. Efficiency profile of four-switch bidirectional converter.

withstand voltage of the super capacitor is relatively low. The parameter of the super capacitor selected in this experiment is 10 F/2.7 V. In order to improve the withstand voltage and capacity of the super capacitor, 4 super capacitors are selected and divided into 2 groups. Each group of capacitors is connected in series to increase the capacitor withstand voltage to 5.4 V, and then two groups of capacitors are connected in parallel to increase the capacity to 20 F. In order to ensure the normal operation of the power management chip, the voltage working range of the super capacitor is set to 2.8 to 5 V. When the voltage of the super capacitor reaches the upper and lower thresholds, the working state of the converter will be changed. The relevant parameters of the equalizer are shown in Table II.

The conversion efficiency of the bidirectional converter, which is the main body of energy conversion, is one of the key factors that determine the equalization efficiency of the equalizer in the entire equalization process. The efficiency of the bidirectional converter in the equalizer is tested when working with different condition. The converter efficiency curve is shown in Fig. 11.

With the increase of the equalizing current, the power of the converter is also increasing. The ratio of the loss to the total power is getting lower, and the efficiency of the converter is continuously improving within a certain range. As shown in Fig. 11, the bidirectional converter has a high conversion efficiency.

The performance of the proposed balancing method is tested under different conditions. Fig. 12 shows part of the working waveform of the equalizer. *G1, G2, G3,* and *G4*, respectively, represent the gate drive waveforms of the four switches of the bidirectional converter.

The equalization curve of the battery pack in the static state is shown in Fig. 13. The initial state of each battery is $V_{B1} = 3.12$ V,

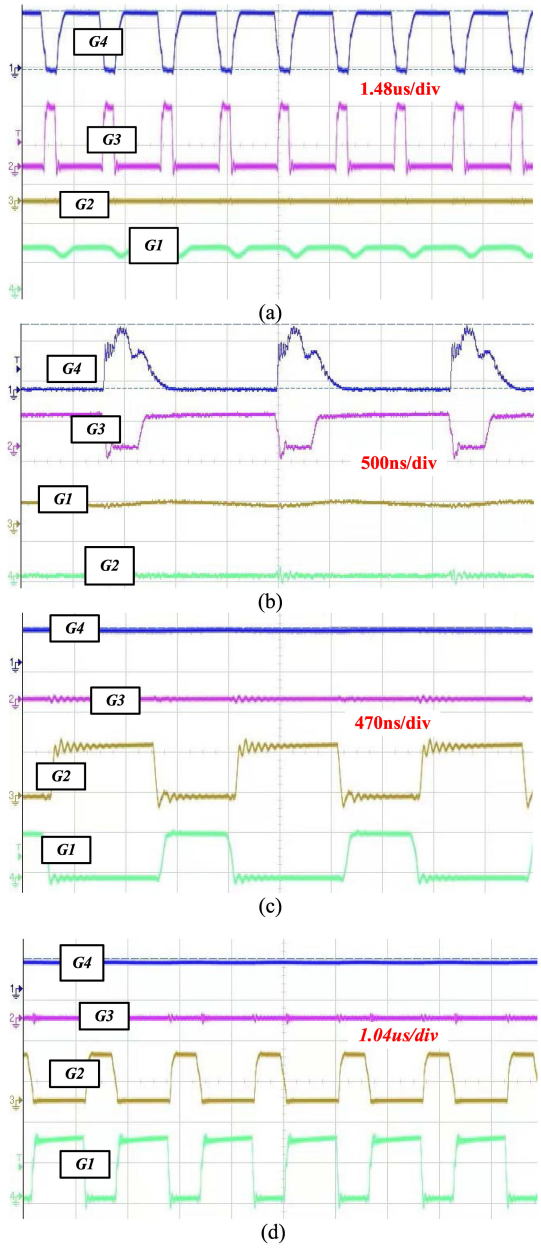

Fig. 12. Experimental waveforms of the converter. (a) Super capacitor discharges battery (4.2−4.07 V). (b) Single battery to charge super capacitor (3.8−4.2 V). (c) Three batteries charge the super capacitor (12−4.2 V). (d) Super capacitor discharges three batteries (4.2−12 V).

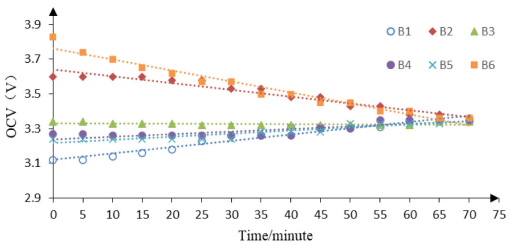

Fig. 13. Battery equalization process under rest state.

TABLE III
COMPARISON OF THE PROPOSED METHOD TO CONVENTIONAL METHODS

Term	Switched capacitor [14]	Single magnetic [18]	Single transformer [17]	*LC* Resonant [22]	Proposed method
Switch	*2 N*	*N*	*N+3*	*N+5*	*2N+4*
Diode	*0*	*0*	*0*	*6*	*0*
Inductor	*0*	*N*	*0*	*1*	*1*
Capacitor	*N*	*0*	*0*	*1*	*1*
Transformer	*0*	*0*	*1*	*0*	*0*
Power switch	*0*	*0*	*2*	*4*	*4*
Cost	Low	Medium	Medium	Medium	Low
Balancing speed	133 min (static balancing, 4 batteries)	150 min (static balancing, 6 batteries)	250 min (static balancing, 12 batteries)	90 min (static balancing, 12 batteries)	65 min (static balancing, 6 batteries)
Efficiency	About 90%	About 60%	About 80.4%	About 93.2%	About 93%

N is the number of cells in the battery string.

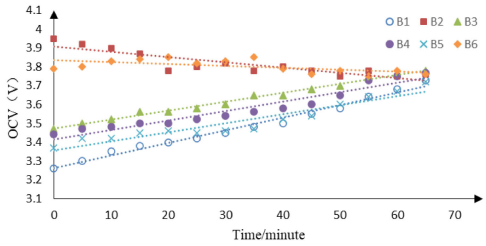

Fig. 14. Battery equalization process under charge state.

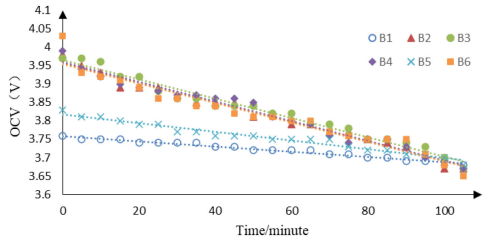

Fig. 15. Battery equalization process under discharge state.

$V_{B2} = 3.60$ V, $V_{B3} = 3.34$ V, $V_{B4} = 3.27$ V, $V_{B5} = 3.24$ V, and $V_{B6} = 3.83$ V.

It can be seen from Fig. 13 that the voltage values of batteries B_2 and B_6 are the highest relative to other batteries, and the voltage value of battery B_1 is the lowest. Batteries B_1, B_2, and B_6 perform the balancing between single cells. Batteries B_3, B_4, and B_5 have similar voltages and are adjacent to each other, and perform the internal group balance. Finally, the battery pack reaches equilibrium about 70 min later.

The equalization curve of the battery pack in the charge state is shown in Fig. 14. The initial state of each battery is: $V_{B1} = 3.26$ V, $V_{B2} = 3.95$ V, $V_{B3} = 3.47$ V, $V_{B4} = 3.44$ V, $V_{B5} = 3.37$ V, and $V_{B6} = 3.79$ V.

As can be seen from Fig. 14, the voltages of batteries B_2 and B_6 are the highest, and the voltage of battery B_1 is the lowest. Batteries B_1, B_2, and B_6 perform the balancing between single cells. B_3, B_4, and B_5 battery voltage values are similar, perform the internal group balance. Under the charge state, the battery pack reaches equilibrium in about 67 min.

The equalization curve of the battery pack in the discharge state is shown in Fig. 15. The initial state of each battery is: $V_{B1} = 3.76$ V, $V_{B2} = 3.98$ V, $V_{B3} = 3.97$ V, $V_{B4} = 3.99$ V, $V_{B5} = 3.83$ V, and $V_{B6} = 4.03$ V.

It can be seen from Fig. 15 that the voltage values of batteries B_1 and B_5 are lower than other batteries, and the voltage values of batteries B_2, B_3, B_4, and B_6 are similar and higher. Batteries B_1, B_5, and B_6 perform the balancing between single cells. Batteries B_2, B_3, and B_4 perform the internal group balance. In the discharging state, the battery pack reaches an equilibrium state in about 110 min.

In order to prove the advantages of the decommissioned battery balancing method proposed in this article, comparisons are made in terms of the number of components, circuit cost, balancing speed, and energy conversion efficiency, as shown in Table III.

In the active balancing process of retired batteries, energy loss mainly comes from the process of energy transfer. Regardless of the battery itself, improving the conversion efficiency of the balancing circuit can reduce the energy loss in a certain sense. In addition, increasing the balancing current can improve the balancing speed within a certain range. In Table III, the switched capacitor type balancing uses capacitor for energy transfer, and the balancing current is relatively small, resulting in a slow equalization speed. The single magnetic type balancing uses inductor as the energy storage element in the balancing process, and the energy is transferred in the form of current, which makes the equalization speed faster. Nevertheless, the presence of more inductive elements in the circuit makes the circuit itself unstable, and the method is less efficient in equalization. The single transformer type balancing has relatively higher circuit loss due to the use of transformer coils for energy transfer. The *LC* resonance type balancing circuit uses a resonant converter with higher conversion efficiency as the main body of the equalizer, so the energy loss is relatively lower. In the method proposed in this article, the main switch works in synchronous rectification mode, which reduces the energy loss during the working process. In addition, larger balancing current and hybrid balancing strategy can increase the speed of balancing. As can be seen in Table III, the balancing method for retired battery packs proposed in this article has higher advantages in terms of balancing speed and conversion efficiency.

VI. CONCLUSION

This article presents an efficient and fast balancing circuit for series retired battery packs. The circuit is mainly composed of a four-switch bidirectional converter, a switch matrix, a super

capacitor energy storage unit, and a control unit. Since the four-switch bidirectional converter is used as the main unit of the equalizer, it can flexibly switch between the boost mode and the buck mode during the equalization process, and transfer the unbalanced energy in the decommissioned battery pack to the super capacitor for storage. Then, the energy in the super capacitor is flexibly distributed to the battery with lower energy through the converter and switch array. At the same time, the *DBSCAN* equalization algorithm is used to cluster the decommissioned battery packs, prioritize the equalization of the nonadjacent single cells in the battery pack, and then balance the internal "battery clusters" between clusters to achieve efficient and fast balancing of the retired batteries in series. Finally, a simulation model was established through the MATLAB/Simulink platform. At the same time, a small experimental platform was designed and produced. Through experiments, the feasibility and effectiveness of the proposed equalization system were proved. And through the comparison with the conventional battery balancing method, the superiority of this method is proved.

REFERENCES

[1] S. Jinlei, L. Wei, T. Chuanyu, W. Tianru, J. Tao, and T. Yong, "A novel active equalization method for series-connected battery packs based on clustering analysis with genetic algorithm," *IEEE Trans. Power Electron.*, vol. 36, no. 7, pp. 7853–7865, Jul. 2021.

[2] Y. Shang, S. Zhao, Y. Fu, B. Han, P. Hu, and C. C. Mi, "A lithium-ion battery balancing circuit based on synchronous rectification," *IEEE Trans. Power Electron.*, vol. 35, no. 2, pp. 1637–1648, Feb. 2020.

[3] K. Lo, Y. Chen, and Y. Chang, "Bidirectional single-stage grid-connected inverter for a battery energy storage system," *IEEE Trans. Ind. Electron.*, vol. 64, no. 6, pp. 4581–4590, Jun. 2017.

[4] S. S. Williamson, A. K. Rathore, and F. Musavi, "Industrial electronics for electric transportation: Current state-of-the-art and future challenges," *IEEE Trans. Ind. Electron.*, vol. 62, no. 5, pp. 3021–3032, May 2015.

[5] C. J. Xie, X. Y. Xu, P. Bujlo, D. Shen, H. B. Zhao, and S. H. Quan, "Fuel cell and lithium iron phosphate battery hybrid powertrain with an ultracapacitor bank using direct parallel structure," *J. Power Sources*, vol. 279, pp. 487–494, 2015.

[6] M. Evzelman, M. M. Ur Rehman, K. Hathaway, R. Zane, D. Costinett, and D. Maksimovic, "Active balancing system for electric vehicles with incorporated low-voltage bus," *IEEE Trans. Power Electron.*, vol. 31, no. 11, pp. 7887–7895, Nov. 2016.

[7] Y. Jiang, J. C. Jiang, C. P. Zhang, W. G. Zhang, Y. Gao, and Q. P. Guo, "Recognition of battery aging variations for $LiFePO_4$ batteries in 2nd use applications combining incremental capacity analysis and statistical approaches," *J. Power Sources*, vol. 360, pp. 180–188, 2017.

[8] S. Jinlei, P. Lei, L. Ruihang, M. Qian, T. Chuanyu, and W. Tianru, "Economic operation optimization for 2nd use batteries in battery energy storage systems," *IEEE Access*, vol. 7, pp. 41852–41859, 2019.

[9] X. Lai, D. D. Qiao, Y. J. Zheng, M. G. Ouyang, X. B. Han, and L. Zhou, "A rapid screening and regrouping approach based on neural networks for large-scale retired lithium-ion cells in second-use applications," *J. Cleaner Prod.*, vol. 213, pp. 776–791, 2019.

[10] S. M. Lukic, J. Cao, R. C. Bansal, F. Rodriguez, and A. Emadi, "Energy storage systems for automotive applications," *IEEE Trans. Ind. Electron.*, vol. 55, no. 6, pp. 2258–2267, Jun. 2008.

[11] Y. J. Xing, E. W. M. Ma, K. L. Tsui, and M. Pecht, "Battery management systems in electric and hybrid vehicles," *Energies*, vol. 4, no. 11, pp. 1840–1857, 2011.

[12] Z. B. Omariba, L. Zhang, and D. Sun, "Review of battery cell balancing methodologies for optimizing battery pack performance in electric vehicles," *IEEE Access*, vol. 7, pp. 129335–129352, 2019.

[13] C. Kim, M. Kim, H. Park, and G. Moon, "A modularized two-stage charge equalizer with cell selection switches for series-connected lithium-ion battery string in an HEV," *IEEE Trans. Power Electron.*, vol. 27, no. 8, pp. 3764–3774, Aug. 2012.

[14] Y. Shang, F. Lu, B. Xia, C. Zhang, N. Cui, and C. Mi, "A switched-coupling-capacitor equalizer for series-connected battery strings," in *Proc. IEEE Appl. Power Electron. Conf. Expo.*, 2017, pp. 1425–1429.

[15] Y. Shang, B. Xia, J. Yang, C. Zhang, N. Cui, and C. Mi, "A delta-structured switched-capacitor equalizer for series-connected battery strings," in *Proc. IEEE Energy Convers. Congr. Expo.*, 2017, pp. 4493–4496.

[16] A. F. Moghaddam and A. Van den Bossche, "A cell equalization method based on resonant switched capacitor balancing for lithium ion batteries," in *Proc. 9th Int. Conf. Mech. Aerosp. Eng.*, 2018, pp. 337–341.

[17] T. H. Phung, A. Collet, and J. Crebier, "An optimized topology for next-to-next balancing of series-connected lithium-ion cells," *IEEE Trans. Power Electron.*, vol. 29, no. 9, pp. 4603–4613, Sep. 2014.

[18] H. Park, C. Kim, C. Kim, G. Moon, and J. Lee, "A modularized charge equalizer for an HEV lithium-ion battery string," *IEEE Trans. Ind. Electron.*, vol. 56, no. 5, pp. 1464–1476, May 2009.

[19] Y. Gong and T. Tang, "Controlling and balancing of lithium battery voltage based on inductance equilibrium method," in *Proc. IEEE Int. Symp. Power Electron. Power Electron., Elect. Drives, Automat. Motion*, 2012, pp. 347–352.

[20] S. Li, C. C. Mi, and M. Zhang, "A high-efficiency active battery-balancing circuit using multiwinding transformer," *IEEE Trans. Ind. Appl.*, vol. 49, no. 1, pp. 198–207, Jan./Feb. 2013.

[21] S. Park, K. Park, H. Kim, G. Moon, and M. Youn, "Cell-to-cell charge equalization converter using multi-winding transformer with reduced number of windings," in *Proc. 8th Int. Conf. Power Electron.*, 2011, pp. 285–290.

[22] M. Kim, J. Kim, and G. Moon, "Center-cell concentration structure of a cell-to-cell balancing circuit with a reduced number of switches," *IEEE Trans. Power Electron.*, vol. 29, no. 10, pp. 5285–5297, Oct. 2014.

[23] X. Tang *et al.*, "Run-to-run control for active balancing of lithium iron phosphate battery packs," *IEEE Trans. Power Electron.*, vol. 35, no. 2, pp. 1499–1512, Feb. 2020.

[24] M. Raeber, A. Heinzelmann, and D. O. Abdeslam, "Analysis of an active charge balancing method based on a single nonisolated DC/DC converter," *IEEE Trans. Ind. Electron.*, vol. 68, no. 3, pp. 2257–2265, Mar. 2021.

[25] Y. Guo, R. Lu, G. Wu, and C. Zhu, "A high efficiency isolated bidirectional equalizer for lithium-ion battery string," in *Proc. IEEE Veh. Power Propulsion Conf.*, 2012, pp. 962–966.

Wang Lujun received the B.S. and Ph.D. degrees from Zhejiang University, Hangzhou, China, in 2008 and 2013, respectively.

He has authored or coauthored more than 30 papers, including one ESI highly cited paper and four invention patents. His current research interests include battery balancing, micro-grid, energy storage systems, and solid-state circuit breakers.

Dr. Lujun is a Reviewer for IEEE TRANSACTIONS ON INDUSTRIAL ELECTRONICS and *Journal of Zhejiang University Science*.

Ke Jinyang received the B.S. degree in electrical engineering from the Hubei University of Technology Engineering and Technology College, Wuhan, China, in 2019. He is currently working toward the M.S. degree with Hubei University of Technology, Wuhan, China.

His main research interests focus on the battery balancing technology, especially on circuit topology and control method.

Zhan Min received the B.S. degree in communication engineering from the Hubei University of Technology Engineering and Technology College, Wuhan, China, in 2020. She is currently working toward the M.S. degree with Hubei University of Technology, Wuhan, China.

Her main research interest focuses on the battery balancing technology.

Tian Aina received the B.S. degree from the China University of Petroleum (East China), Beijing, China, in 2013, and the Ph.D. degree from the Harbin Institute of Technology, Harbin, China, in 2019.

She is currently working with the School of Electrical and Electronic Engineering, Hubei University of Technology, Wuhan, China. Her current research interests include new energy related technology, power system analysis, and control and battery safety.

Wu Tiezhou biography not available at the time of publication.

Zhang Xiaoxing biography not available at the time of publication.

Jiang Jiuchun (Senior Member, IEEE) was born in Jilin Province, China. He received the B.S. degree in electrical engineering and the Ph.D. degree in power system automation from Northern Jiaotong University, Beijing, China, in 1993 and 1999, respectively.

His research interests include battery application technology in electric vehicles and energy storage system, and electric vehicle charging stations.

Dr. Jiuchun received the National Science and Technology Progress 2nd Award for his work on EV bus system, and the Beijing Science and Technology Progress 2nd Award for his work on EV charging system.